Breakwater Reinforcement Method against Large Tsunami

Hiroshi Matsushita

Nikken Kogaku Co., Ltd., Japan

Abstract

The Tohoku-Pacific Ocean Earthquake which occurred in March 2011 generated the huge tsunami of more than 10 m. The tsunami attacked the Pacific coast of Japan several times and collapsed many breakwaters. Furthermore big typhoons which generate extremely big waves higher than the design one for maritime structures have sometimes appeared recently. The frequent appearance of the big typhoons may be affected by climate change due to global warming. The extremely big waves have caused serious damages to breakwater. Therefore, new methods for breakwater reinforcement are required to develop.

Previously the heightening of rubble mound in the rear part of the breakwater was employed as a reinforcement method for upright breakwaters. However, because the heightening of the rear mound may expand the width of the mound to the waterway, the heightening is not preferable for safety navigation in the waterway. The stones of the rubble mound also may be carried into the waterway by the flow induced by the tsunami overflow.

We have developed a counter-weight type block (named SUBPLEO FRAME) which can be expected to exert large sliding resistant force in spite of small cross-section. This block shows a horizontally square shape with a large rectangular hole in the center, and stones are packed in the hole. The very large resistant force caused by the friction among the stones reduces the size of the cross section of the block. In addition, the model tests show that the blocks are stable against the tsunami overflow.

Model tests on pulling the block were carried out to evaluate the friction factor of the counter-weight type block. Additionally hydraulic model experiments on the motion of the block were conducted to confirm the validity of the value of friction factor. The model tests for the friction have derived 0.75 as the value of the friction factor for design. The hydraulic model experiments have concluded that the blocks designed by the friction factor of 0.75 are sufficiently stable.

A tsunami overflow experiments were performed to check the stability performance of the counter-weight type block in comparison with the mound heightening. As the result, the counter-weight type block shows its stability against the tsunami overflow is quite good.

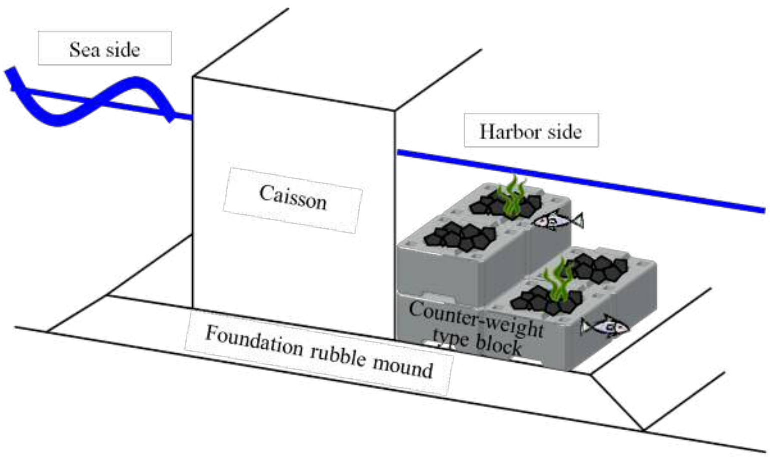

Keywords: tsunami, extremely big wave, breakwater reinforcement, counter-weight type block, friction factor, tsunami overflow

1. INTRODUCTION

At 2:46 p.m. on March 11, 2011, the great earthquake of M=9.0 occurred at about 24*km* deep under the seabottom in the Pacific Ocean off Sanriku of Japan. The earthquake has been named the Tohoku-Pacific Ocean Earthquake. About 30 minutes later than the earthquake, the first tsunami reached the Pacific coast of Japan, and the tsunamis higher than 10m attacked there several times. Many breakwaters were damaged by these tsunamis. Figure 1 shows the damage state of the breakwater at Hachinohe port in Aomori Prefecture. As shown in Figure 1, a half of the central part of the north breakwater were removed and almost all caissons of the wing part of the breakwater were scattered by the tsunami.
Figure 2 shows the breakwater at Tsuruga port in Fukui Prefecture. A caisson was damaged by extremely large storm waves generated by the migrating depression on April 3, 2012. The caisson of 3000*tf* was moved 15*m* backward. Figure 3 shows the time histories of the significant wave height and period observed at that time. The highest wave height in the time history reached more than 6*m* and it was more than twice higher than the design wave of 2.67*m*. The period of the highest wave was also longer than that of the design wave. Such events of abnormally large waves over the design one seem to be more frequent recently. The occurrence of the abnormal waves may be affected by the global climate change.
In Japan, the extreme wave of the return period of 50 years is normally employed as the design one for coastal and offshore structures. The design waves for the existing breakwaters in Japan were estimated from observed and hindcasted waves in the storms which occurred in the mid-twenty century, because most of the breakwaters were built 30 to 40 years ago. If the

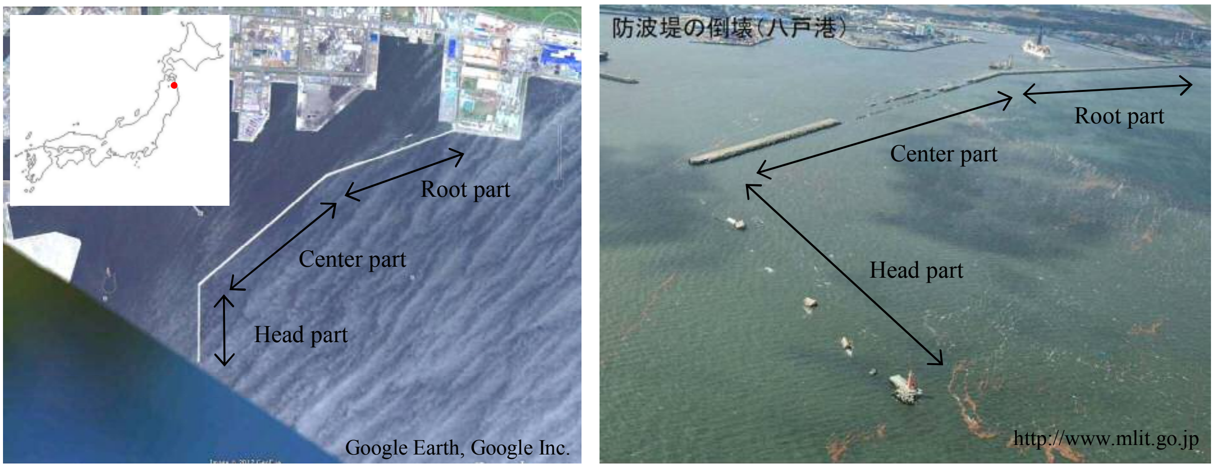

(a) Before Tsunami (b) After Tsunami

Figure 1. Breakwater of Hachinohe Port

Figure 2. Breakwater of Tsuruga Port

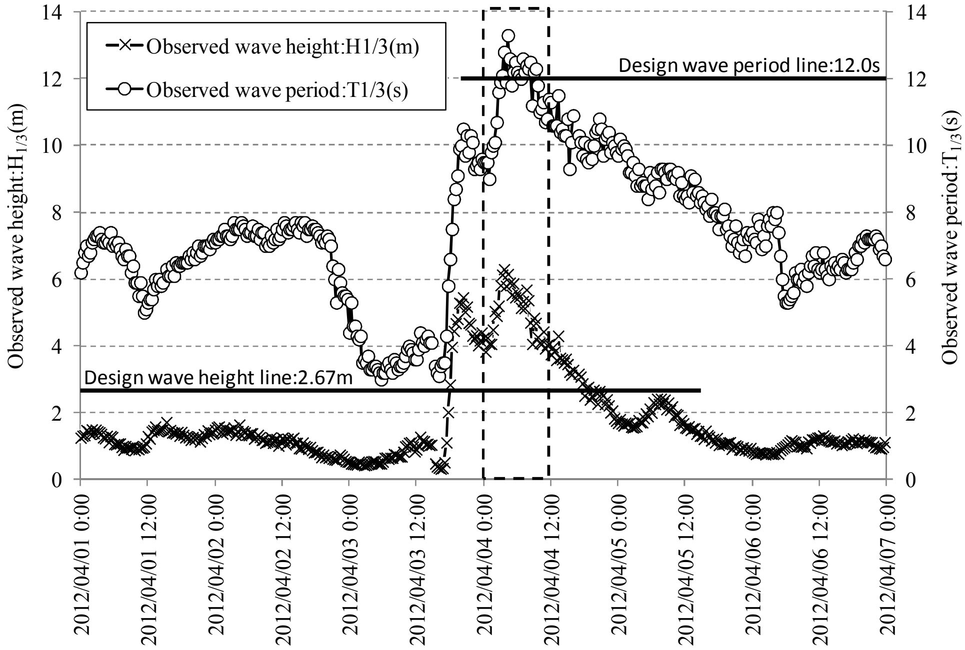

Figure 3. Time histories if height and period of observed significant wave

extremely large waves of recent years or the large tsunami like the Tohoku-Pacific Ocean Earthquake hit the breakwaters, they exert a high risk to the breakwater damage. Therefore the breakwater reinforcement is required, but the large-scale improvement of the present breakwaters is costly and influential to the surrounding ecosystem. Simple and low-cost techniques effective on the increase of the breakwaters resistance are widely demanded.

We have proposed a new counter-weight type concrete block named *SUBPLEO FRAME* (SPF; Patents pending in collaboration with DPRI, Kyoto Univ.) which has a rectangular hole filled by stones. The stones inside the hole exert large frictional force to resist the horizontal movement of the block. The SPF is placed in a rear part of a breakwater caisson to suppress the caisson from sliding backward.

The present paper describes the features of the SPF, the experiment on its frictional factor, the hydraulic tests on its stability and the design procedures of the SPF. In addition, the tsunami overflow scoured the rubble mounds in the rear parts of the breakwaters in the Eastern Japan Great Earthquake Tsunami Disaster and the scouring may affect the stability of a caisson, although it is uncertain for now. The hydraulic experiments were also carried out to check the effect of the SPF on the stability of the rubble mound.

2. FEATURES OF THE SUBPLEO FRAME

Armor and foot protection blocks are conventionally placed on the rubble mounds of breakwaters. Their purpose is only to protect the rubble mound, but not to increase the resistant force of breakwaters. These blocks are almost flat shape without holes (normal block). The friction is produced only between the blocks and rubble mound.

Figure 4 shows the shape of the concrete frame of the SPF newly proposed. The SPF can be placed on another one. The rectangular hole of the SPF is filled by stones. When the SPF starts to move, big shearing force is created between the stones in the hole and rubble mound as shown in Figure 5. Therefore, the SPF is stable compared with other normal block of same weight.

Figure 6 shows a installation image of the SPF to improve the sliding stability of a caisson. As shown in Figure 6, the SPFs are placed in the rear part of the caisson to suppress the sliding and overturning of the caisson and they were unnecessary to widen the rubble mound at their installation. The blocks of SPF can be expected to be stable without heightening and widening the rubble mound shown in Figure 7.

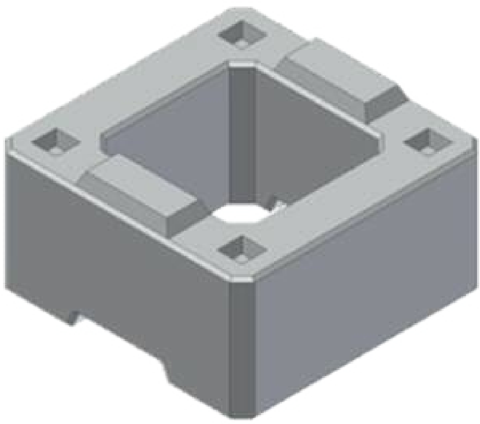

Figure 4. *SUBPLEO FRAME* perspective view

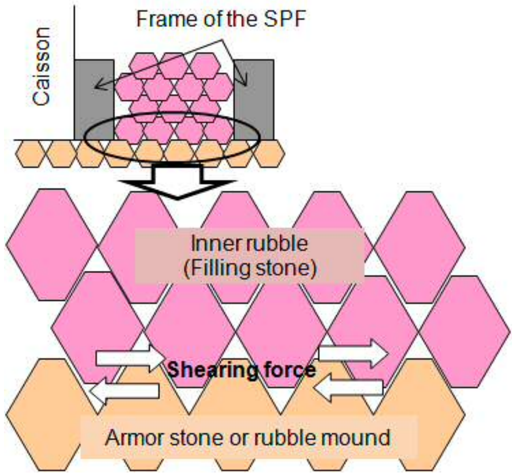

Figure 5. Mechanism of shearing resistance

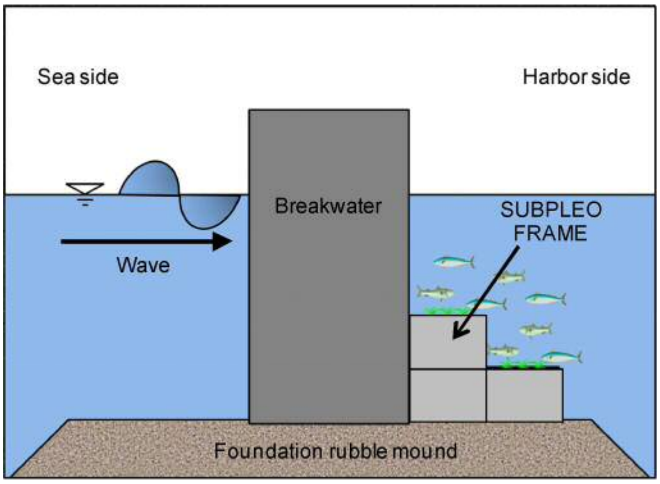

Figure 6. Image of the SPF

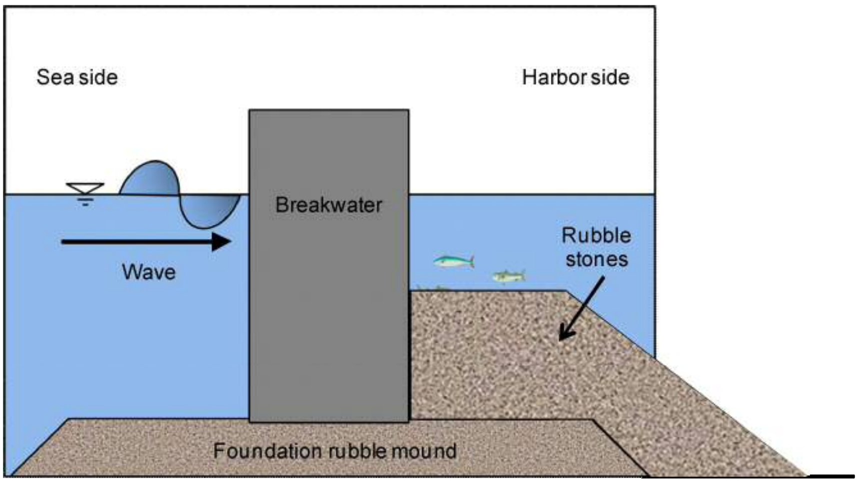

Figure 7. Image of the heightening and widening rubble mound（OCDI, 2009）

The stones inside the SPF can be expected to be effective on water purification and seaweed plantation. The natural stones in a harbor has already been confirmed to be effective on water purification inside the harbor as the stone bed with biofilm (Horie et al., 1995). In addition, if the water depth becomes shallow, alga zone is likely formed on the block and improves the biological environment in a harbor.
Armor block with a small hole is widely used in the world to prevent scatter of mound stones. The hole is made in order to stabilize the block itself by the reduction of the uplift pressure. Therefore, the stones are not packed in the hole.

3. EXPERIMENT ON FRICTION FACTOR OF THE SPF

The SPF exerts resistant force induced by the friction between rubble stones in a hole of the SPF and the rubble mound, but the resistant force should be estimated for the practical design. The resistant force can be predicted simply through the friction factor. The experiments were carried out to determine the value of the factor. This chapter describes some details of the experiments.

3.1 Method and Condition of Experiments

Figure 8 shows block models used in experiments. The left and right blocks in the upper photo in the figure correspond to the normal block model without a hole and the model of the SPF itself, respectively. The lower photo shows the state of the SPF packed by the stones. The size of each block is listed on Table 1. The models of the normal block and the SPF are adjusted to become nearly the same weight each other. The model scale corresponds to 1/5 if the actual size is given by $2m$ long×$2m$ wide×$1m$ high. Figure 9 shows a overview of the

Figure 8. Block models

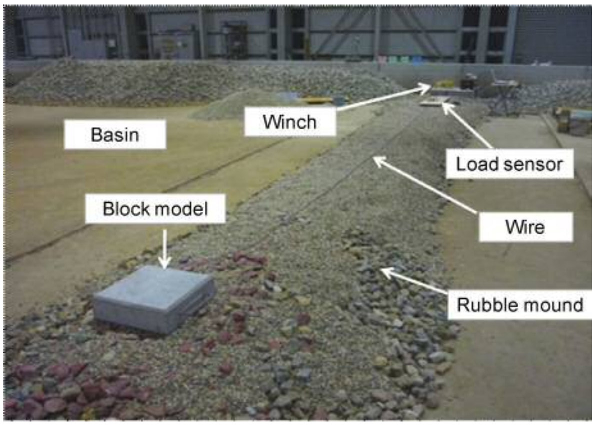

Figure 9. Overview of the experiment

Table 1. Size of block models

		Normal flat block (no hole)	SUBPLEO FRAME :SPF
Length		40cm	40cm
Breadth		40cm	40cm
Height		13cm	20cm
Hole	Length	-	24cm
	Width	-	24cm
Mass		45.8kg	46.7kg

Table 2. Size of stone materials

	Under layer stones (rubble mound)		Inner stones of the SPF	
Color	Red		Yerrow	
Mass	122.6g		135.4g	
Density	2.7g/cm^3		2.5g/cm^3	
Maximum length:L	7.0cm		7.1cm	
Maximum width:W	4.7cm		5.1cm	
Thickness	2.7cm		3.4cm	
W/L	0.67		0.72	
Averaged diameter:Da	5.4cm		5.2cm	

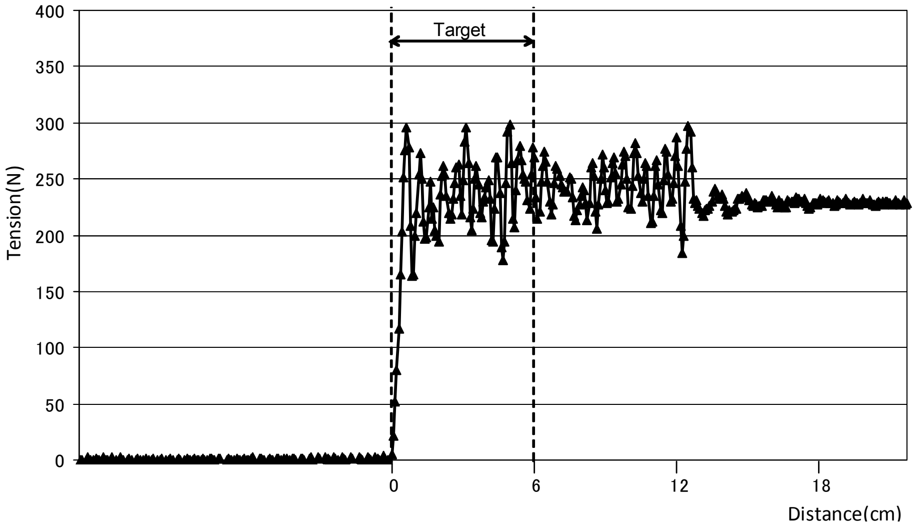

Figure 10. Example of variation of measured tension by load sensor

experimental set-up. A rubble mound was formed with a thickness of 40*cm* in the dry basin. Block models were set on the rubble mound and pulled by a small electric winch at a constant speed. A variable tensile force of the wire (sliding resistant force) was measured by a load sensor inserted between the wire and winch.

The size of rubble mound stones for the breakwaters is usually uniform for the layers near mound surface. The model mound was constructed by small stones, but the top layer was covered by three layers of the stones same as packed inside the SPF. The sizes of rubble stones employed for the mound and for packing in a hole of the SPF are indicated on Table 2. Each value on Table 2 are mean values of those 50 pieces. The stones for the mound and in a hole of the SPF are painted in different colors to distinguish them in the experiment.

An allowable value of the expected sliding distance in a life time of a breakwater has been proposed as the value less than 30*cm* for design in Japan (Shimosako and Takahashi, 1998). In this experiment the value of 30*cm* was assumed as an allowable sliding distance. The value in the model can be calculated to 30*cm*/5=6*cm* as the model scale of 1/5. Figure 10 shows an example of measured tension of the pulling wire, and the vertical and horizontal axes in the figure indicate the tension and sliding distance, respectively. The wire was pulled at initial tension of about 10*N* to prevent loosening, and the block models were pulled by the winch after the initial value was adjusted to zero.

The friction factor μ of the block SPF can be calculated the following Eq.(1):

$$\mu = F/mg \tag{1}$$

where F, m and g represent the tensile force of the wire, the total block mass including the concrete frame and inner stones, and the gravitational acceleration, respectively.
The pulling model tests were repeated five times in the same condition. The average value of five measured tensile forces was employed as the value of F in the calculation of the friction factor.
It is thought that the measured tensile force is composed of two different friction forces at the concrete frame and the stones in the hole. Therefore, the tensile force can be expressed by Eq.(2).

$$F = \mu_c m_c g + \mu_s m_s g \tag{2}$$

where the subscripts c and s denote the concrete frame and the stones in the hole. The friction factor of the stones in the hole can be evaluated by using Eq.(3) transformed from Eq.(2), if the value of the friction factor of the concrete frame can be obtained.

$$\mu_s = \frac{F - \mu_c m_c g}{m_s g} \tag{3}$$

The value of the friction factor of the concrete frame can be estimated by the pulling test of the concrete frame without the stones in the hole.

3.2 Experimental Result

Case1 indicates the test for the normal block, and Case2 and 3 indicate the tests for the SPF without and with the rubble stones in a hole. Figure 11 shows the state of the pulling test of Case2.
The average value of five same tests was used for the calculation of the friction factor because the tests for the stones vary widely even in same experimental conditions. The time variations of average tensile forces of five same tests are shown in Figure 12(a). The vertical and horizontal axes in the figure indicate the tension and the sliding distance, respectively. The friction factors were calculated by substituting the average tensile forces into Eq.(1) and the calculation results are shown in Figure 12(b). The average tensile forces of Case3 for the SPF are about twice larger than those of Case1 for the normal block, as shown in Figure 12(a). On the other hand the same figure shows that the tensile forces of Case2 are little bit larger than those of Case1. This means that the friction force between the stones in the hole and the mound stones is quite large and the empty hole is also little effective on the increase of the

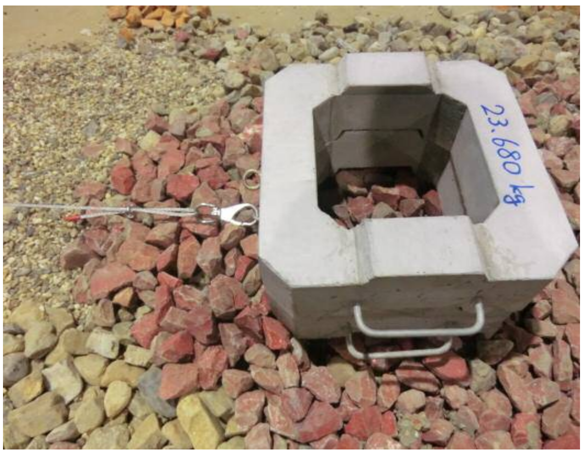

Figure 11. Pulling test of Case2

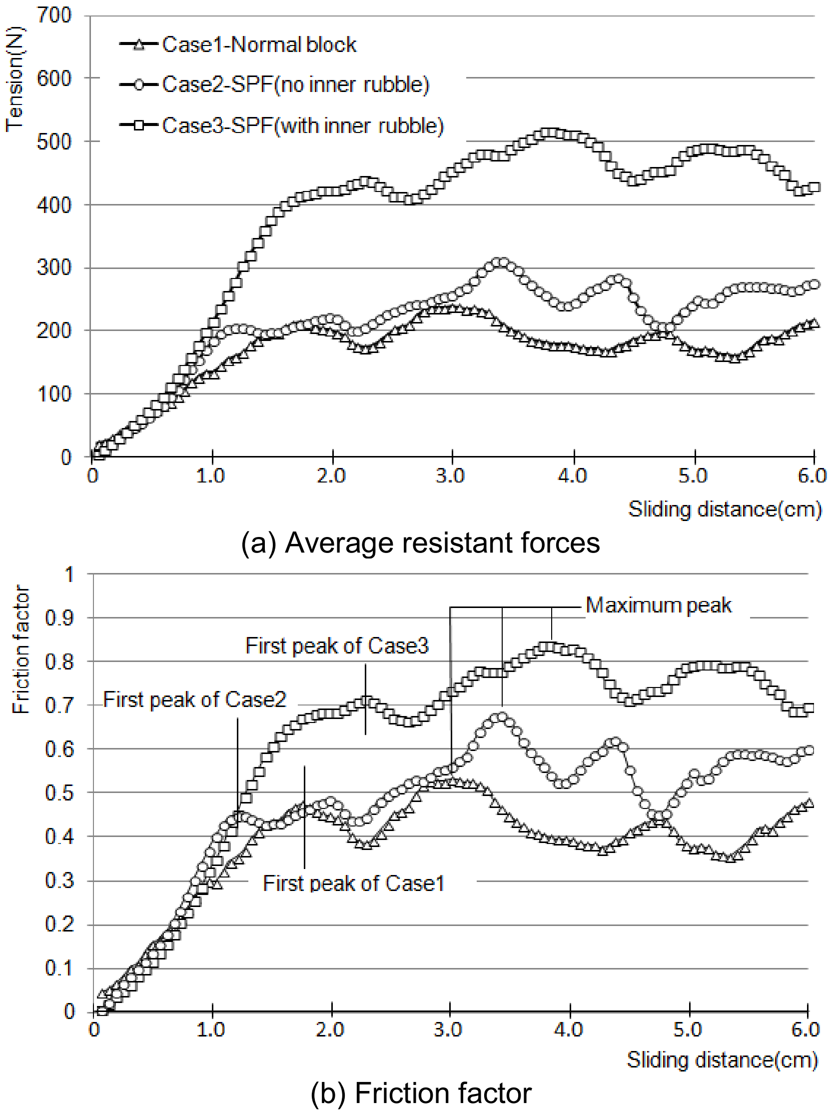

Figure 12. Experimental results

resistant force, because the hole catches the stones on the mound.

The friction factors in almost steady state vary 0.4 to 0.5 in Case1, 0.5 to 0.6 in Case2 and 0.7 to 0.8 in Case3, respectively. The maximum friction factor becomes 0.53 in Case1. The value of 0.53 is slightly small compared with the conventional value of 0.6 (OCDI, 2009) as the friction factor between concrete and rubble. On the other hand, the maximum value of the friction factor is 0.68 in Case2 and 0.83 in Case3. These values are large compared with the conventional value of 0.6. The friction factor of the stones was obtained as μ_s=1.29 by substituting the maximum value of 0.68 into Eq.(3) as the value of μ_c. The value of 1.29 is quite large compared with the conventional friction factor of 0.8 (OCDI, 2009) among stones. Though the conventional value of 0.8 has been derived as the friction factor between two stones, the value of 1.29 was calculated as the friction factor between two groups of stones.

3.3 Determination of Design Friction Factor

The previous section discussed the maximum values of the friction factor, but it is difficult to employ these values in the actual design because the maximum values are the average one of the original five same tests. The variation of the friction factor after the first peak can be regarded as steady state. In the steady state the distribution of the friction factor in Case3 was

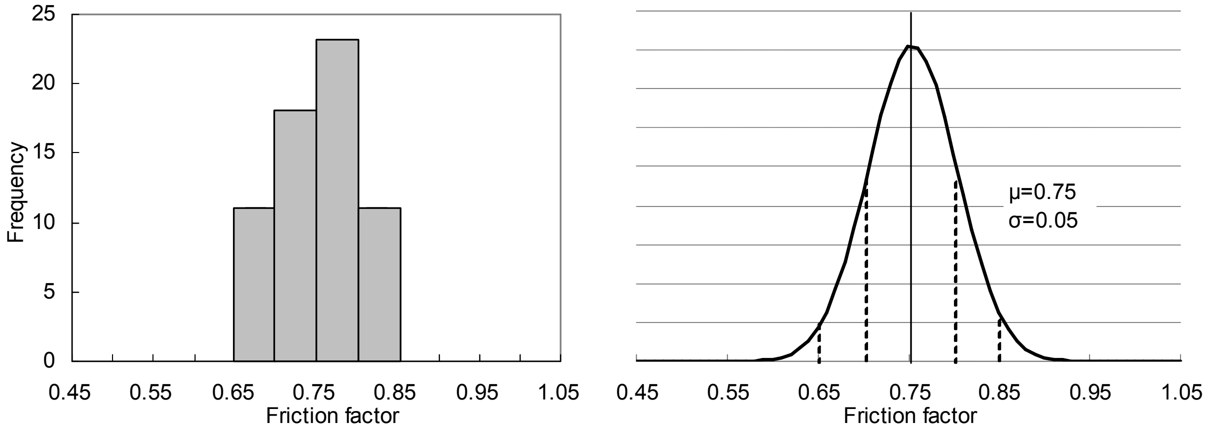

Figure 13. Histogram and normal distribution of Case3

checked. Consequently, the friction factors were expressed as the normal distribution with the mean value of 0.75 and the standard deviation of 0.05. The left and right figures in Figure 13 shows the histgram and the normal distribution of the friction factor in Case3. The data distributes between 0.65 and 0.85, and the standard deviation of 0.05 is small.
The value of 0.75 has been determined to employ as the design friction factor of the SPF μ_{SPF} with stones in a hole.

3.4 Design Procedures (*Calculation of Resistant Force against Sliding*)

When we employ the SPF to reinforce the coastal structures like breakwaters, we must know the resistant force corresponding to the size of the SPF. This section explains how to estimate the resistant force against sliding by using the value of 0.75 as the design friction factor.
As an example, the calculation was performed for just one 20*t*-type. The dimension and calculation specification are shown in Figure 14 and Table 3, respectively.

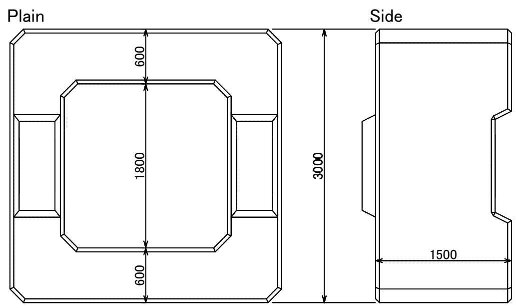

Figure 14. Dimension of 20t-type

Table 3. Calculation specification

Size	20t-type
Concrete volume : V	8.471 m^3
volume of a hole : V_h	4.793 m^3
Concrete density : ρ_c	2.3 t/m^3
Stone density : ρ_s	2.6 t/m^3
Sea water density : ρ_w	1.03 t/m^3
Gravity acceleration : g	9.8 m/s^2

First, the mass of the inner stones M_s is calculated as the stone mass in the hole by Eq.(4) where V_h , φ and ρ_s represent the volume of the hole, the porosity of the stones and the stone density. The value of 50% was employed as the porosity. Next, the underwater weight of SPF W_{w_SPF20t} is calculated by Eq.(5). Finally, the resistant force F_{SPF20t} can be obtained by multiplying μ_{SPF} =0.75 to the underwater weight as Eq.(6).

$$M_s = V_h \cdot \varphi \cdot \rho_s \tag{4}$$

$$W_{w\_SPF20t} = W_c + W_s = M_c \cdot {(\rho_c - \rho_w)}/{\rho_c} \cdot g + M_s \cdot {(\rho_s - \rho_w)}/{\rho_s} \cdot g \tag{5}$$

$$F_{SPF20t} = W_{w\_SPF20t} \cdot 0.75 \tag{6}$$

where M and W represent the mass and the weight, and the subscripts c and s denote the concrete and the stone, respectively.
Eqs.(7), (8) and (9) show the calculated results.

$$M_s = 4.793 \cdot 0.5 \cdot 2.6 = 6.23\,t \tag{7}$$

$$W_{w\_SPF20t} = 8.471 \cdot 2.3 \cdot {(2.3-1.03)}/{2.3} \cdot 9.8 + 6.23 \cdot {(2.6-1.03)}/{2.6} \cdot 9.8 = 142\,kN \tag{8}$$

$$F_{SPF20t} = 142 \cdot 0.75 = 106\,kN\ (106kN/3m = 35kN/m) \tag{9}$$

4. HYDRAULIC MODEL EXPERIMENT

Hydraulic model experiment was carried out to verify the stability of the SPF and confirm the validity of the friction factor.

4.1 Outline of Experiment

The experiments were conducted in a wave basin of 45m wide, 30m long and 1m deep of Ujigawa Open Laboratory, Disaster Prevention Research Institute, Kyoto University. The basin is shown in Figure 15. A channel of 0.6m wide and 2m long was made by the metal

Figure 15. Wave basin

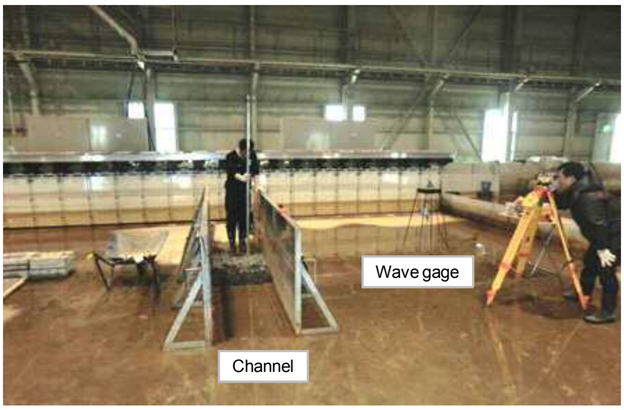

Figure 16. Channel

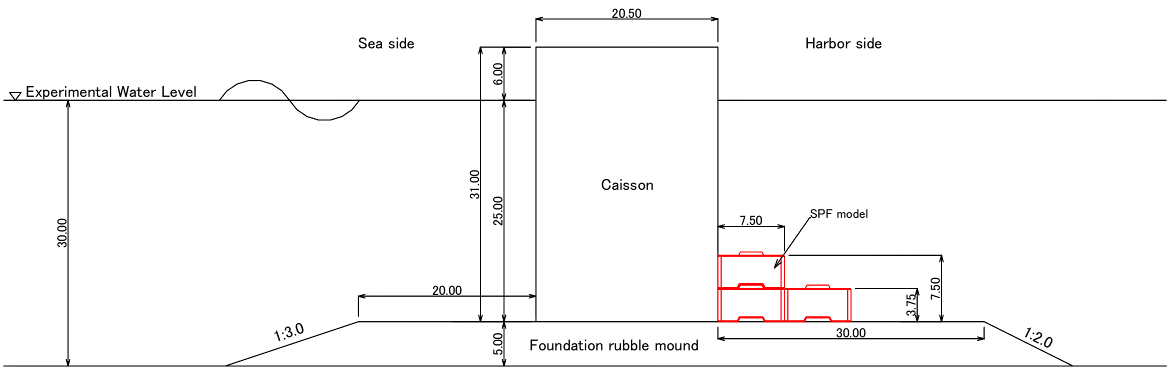

Figure 17. Cross-sectional view (unit:cm)

plates in the basin and a breakwater model was set up in the flat channel as shown in Figure 16. A cross section of the breakwater is shown in Figure 17. The mound slope and width in the sea side were 1:3 and about 20*cm*, respectively. In the harbor side they were 1:2 and about 30*cm*. The water depth was 30*cm*. Figure 18 shows the models of the caisson and SPF and their dimensions are listed on Table 4. The horizontal wave force P_H and uplift force P_U were calculated in the Goda's formula. The bearing force of the caisson F_c and the safety factor $S.F.$ were calculated by Eqs.(10) and (11).

$$F_c = \mu_c \cdot (W_c - P_B - P_U) \tag{10}$$

$$S.F. = F_c / P_H \tag{11}$$

where μ_c, W_c and P_B denote the friction factor between caisson and rubble mound, the weight of caisson and the buoyancy.

The caisson model was designed to satisfy the safety factor of 1.0 in Eq.(11) under the action of the significant wave of 10*cm* high and 1.2*s* in period in a state of only caisson.

The square hole of the SPF is 4.5*cm* long and wide. The mass of the block model with rubble stones is about 400*g* per piece. These values are given as the model scale of 1/40 of the actual 20*t*-type SPF. The two different runs of random waves of the Bretschneider-Mitsuyasu spectra were generated in the experiments. In each run, 300 waves were operated. Though the significant waves in two runs are same as 10*cm* in height, but different in period such as 1.5*s* and 2.0*s*. As shown in Figure 16, the waves were observed by the wave gage outside of the channel.

Figure 19 shows various cross-sections of breakwater employed in the experiments. Large stones of about 120*g* are piled behind the breakwater in Case2. Total mass of large stones is

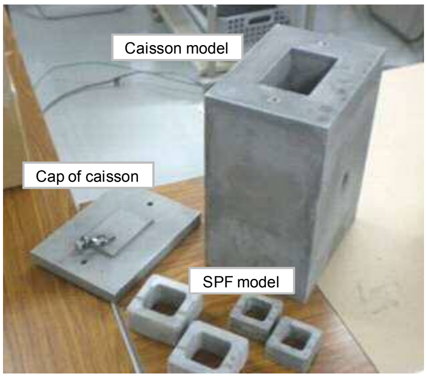

Figure 18. Caisson and SPF models

Table 4. Size of block model

		Caisson	SPF
Height		31cm	3.75cm
Length		20.5cm	7.5cm
Breadth		15cm	7.5cm
Hole	Length	-	4.5cm
	Width	-	4.5cm
Mass		18.11kg	305g

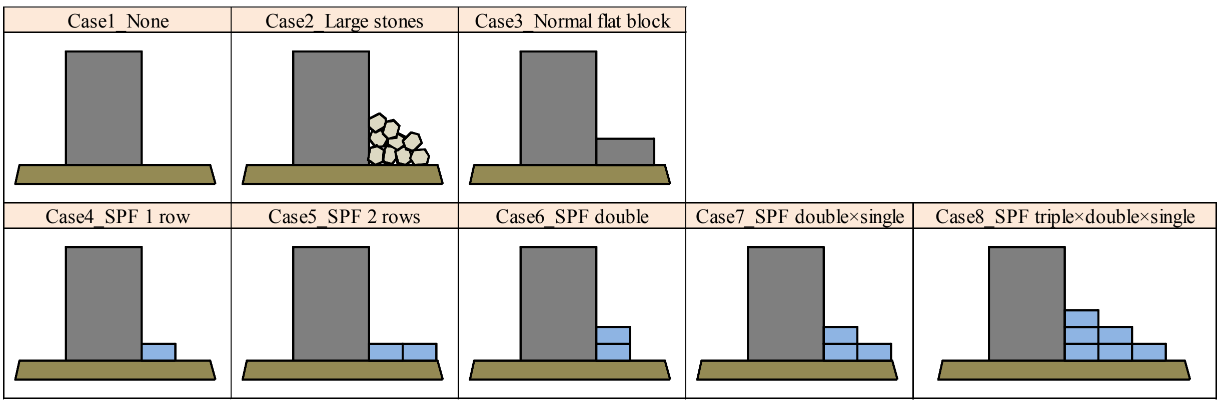

Figure 19. Experimental cases

nearly same as that of 2 SPFs blocks with inner stones. The normal flat block in Case3 is a rectangular shape of 13*cm* long, 13*cm* wide and 4.5*cm* high and its mass is 1780*g* equivalent to that of 4.5 SPFs with inner stones. Case4 to 8 are for the SPF with inner stones.
Three caissons were placed parallelly with the gap of 5cm on the rubble mound as shown in Figure 20. Conditions of the rubble mound may be different at the position of a caisson because the rubble mound is made by natural stones. The wave condition may also be different at position to position because of the affection of the side wall. Therefore, the caisson was rotated in the order of the left, center and right.

Figure 20. Rotation of three positions (Taken from the harbor side)

4.2 Experimental Result

The hydraulic model experiments were carried out for the model of the SPF 20*t*-type, where the model scale of 1/40 was employed. The results of the experiments are summarized on Table 4. The friction factor μ_c between the caisson and rubble mound was employed as 0.6 in the calculation of the resistant force. The shortfall of resistant force R_m is calculated by (P_H - F_c), and means the resistant force which the SPF should incur. The sliding distance was observed in the photograph taken from directly above of the caisson with the steel tape measure. An allowable sliding distance is set as 30*cm*/40=7.5*mm*, considering the allowable value of 30*cm* in prototype. The mark of "OK" means that the sliding distance in the experiments satisfies the allowable value. The mark of "NG" is given when the sliding distance exceeds the allowable one. All results are given by the average value at three different positions (left, center and right).

Table 4. Results of the hydraulic model experiments (three times average)

		Set period $T_{1/3}$(s)	Acted Wave			Bearing force of Caisson : Fc (N/cm)	Wave force : P_H (N/cm)	Safety factor *S.F.*	Shortfall : R_m (N/cm)	Sliding distance :y(mm)		y/$H_{1/3}$	SPF20t-type Calculated value of resistant force : $Rcal$ (N/cm)	$R_m/Rcal$
			$T_{1/3}$ (s)	$H_{1/3}$ (cm)	H_{max} (cm)									
Case1	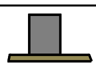	1.5	1.53	10.0	17.9	3.33	4.17	0.80	0.84	24.5	NG	0.244	-	-
		2.0	2.00	10.7	20.0	3.06	5.44	0.57	2.37	46.0	NG	0.428		-
Case2	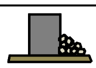	1.5	1.54	10.1	18.3	3.32	4.25	0.78	0.93	13.7	NG	0.135	-	-
		2.0	2.00	10.7	20.0	3.06	5.44	0.57	2.37	46.0	NG	0.428		-
Case3	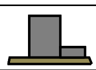	1.5	1.53	9.9	18.2	3.32	4.27	0.78	0.96	6.0	OK	0.061	-	-
		2.0	2.06	11.1	19.9	3.05	5.47	0.56	2.41	24.0	NG	0.216		-
Case4	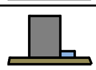	1.5	1.53	10.0	17.5	3.34	4.09	0.82	0.75	3.7	OK	0.037	0.225	3.3
		2.0	2.00	10.7	20.0	3.06	5.44	0.57	2.37	15.7	NG	0.146		10.5
Case5	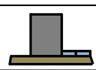	1.5	1.53	9.9	18.2	3.32	4.27	0.78	0.96	3.3	OK	0.034	0.450	2.1
		2.0	2.06	11.1	19.9	3.05	5.47	0.56	2.41	5.7	OK	0.051		5.3
Case6	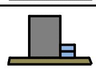	1.5	1.53	10.0	17.5	3.34	4.09	0.82	0.75	0.0	OK	0.000	0.450	1.6
		2.0	2.06	11.1	19.9	3.05	5.47	0.56	2.41	4.0	OK	0.036		5.3
Case7	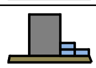	1.5	1.53	9.9	18.2	3.32	4.27	0.78	0.96	2.7	OK	0.027	0.674	1.4
		2.0	2.02	11.0	20.5	3.03	5.60	0.54	2.57	5.7	OK	0.052		3.8
Case8	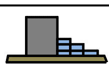	1.5	1.54	10.1	18.3	3.32	4.25	0.78	0.93	1.0	OK	0.010	1.349	0.6
		2.0	2.02	11.0	20.5	3.03	5.60	0.54	2.57	5.0	OK	0.046		1.9

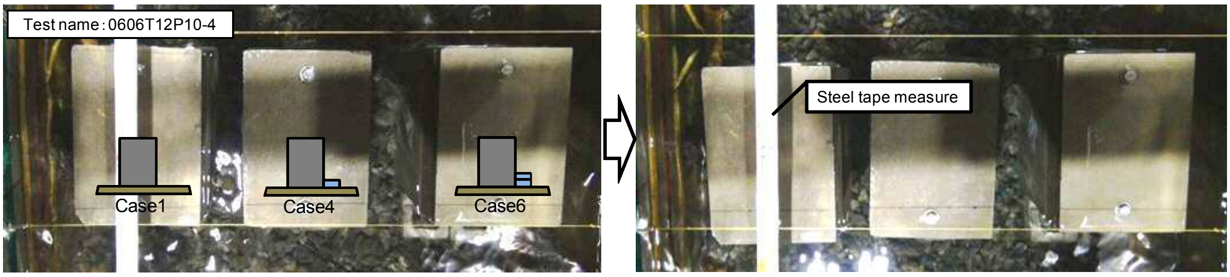

Figure 21. Sliding displacement of caissons (Left:Before wave action, Right:After wave action)

The sliding distances of the caissons in Case1, 2 and 3 were very large, but sliding distance of the caissons with the SPFs in its rear mound were almost within the allowable distance. It is thought that the caisson of Case1, 2 and 3 largely slid due to the insufficient resistant force. On the other hand, it is supposed that the SPF is effective on the increase of the resistance force.
Figure 21 shows the initial state of three different caissons of Case1(left), Case4(center) and Case8(right) in the left photo and the final state after sliding in the right photo. The random waves of $T_{1/3}$=1.44*s* and $H_{1/3}$=10.9*cm* were generated. After the wave action, Three caissons in Case1, 4 and 6 moved backwards by 20cm, 9cm and 3cm, respectively. It is understood that the more number of the SPF is, the smaller the sliding distance is.
Figure 22 shows the variation of non-dimensional sliding distance $y/H_{1/3}$ to the experimental cases, where y denotes the average sliding distance at three different positions in the experiments. The comparison of the sliding distance is made among Cases2, 3 and 4. In Case2, large stones are placed in the rear part of a caisson and in Case 3 a normal flat block is placed in same part. In Case4, one block of SPF is placed behind a caisson. In spite of the materials placed behind the caisson of Case2 and 3 are 2 and 4.5 times as weight as the SPF with inner stones of Case4 respectively, the sliding distance of Case4 is smallest. This means that the SPF can exert quite large resistant force. The large resistant force depends on the stones packed in the central hole of the SPF.

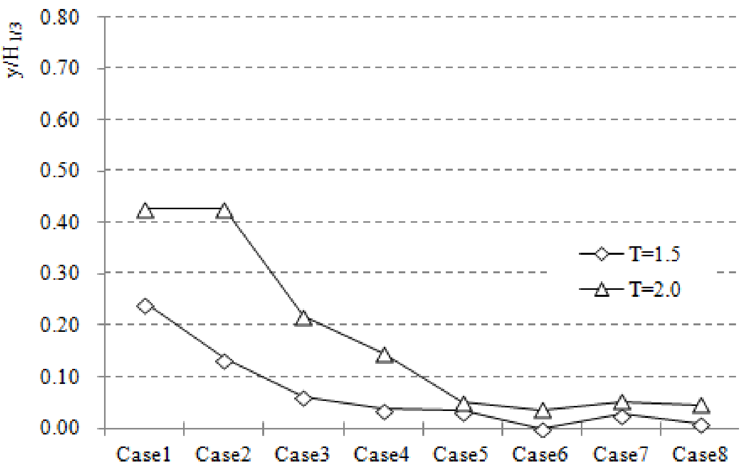

Figure 22. Relationship between the sliding distance and significant wave height

4.3 Comparison with Calculation Value

Rcal for Case4 to 8 in Table 4 represents the resistant force of the SPF which was calculated by the design friction factor of 0.75 and the rightmost column shows the non-dimensional necessary resistant force $R_m/Rcal$.
The sliding distance of Case4 in the wave period of 2.0s was 15.7*mm* and it much exceeded the allowable distance of 7.5*mm*. The force about 10 times larger than *Rcal* was loaded to the

SPF since $R_m/Rcal$ at that time was 10.5. On the other hand, the value of $R_m/Rcal$ in the period of 1.5s was reduced to 3.3 for the same case, because the experimental wave was small. The sliding distance becomes 3.7mm and is smaller than the allowable value of 7.5mm. Considering other all experimental results, the sliding distance satisfies the allowable value if the value of $R_m/Rcal$ is less than about 5. Taking it into account that the wave pressure acting on the caisson in the experiments may be smaller than the calculated one because of the gap between the caissons and the expected sliding distance in life time of a caisson should satisfy the allowable value. The necessary number of SPF should be determined under the condition of $R_m/Rcal$<1.0.

5. TSUNAMI OVERFLOW EXPERIMENT

The scouring of rear rubble mound of a caisson by the tsunami overflow is listed as one of the causes of breakwater collapce in the 2011 Tsunami, as shown in Figure 23. Rubble mound behind the breakwater was scoured by the flow and eddy produced by the tsunami overflow, and finally, it is presumed that the caisson is slid through the reduction of the bearing capacity decrease of the rubble mound.
The tsunami overflow experiments were carried out to verify the adaptability of the SPF for the protection of rubble mound from scoring. A solitary wave was generated for the experiments. The mound heightening method was also verified in the experiments, and their applicability were checked through the experiments.

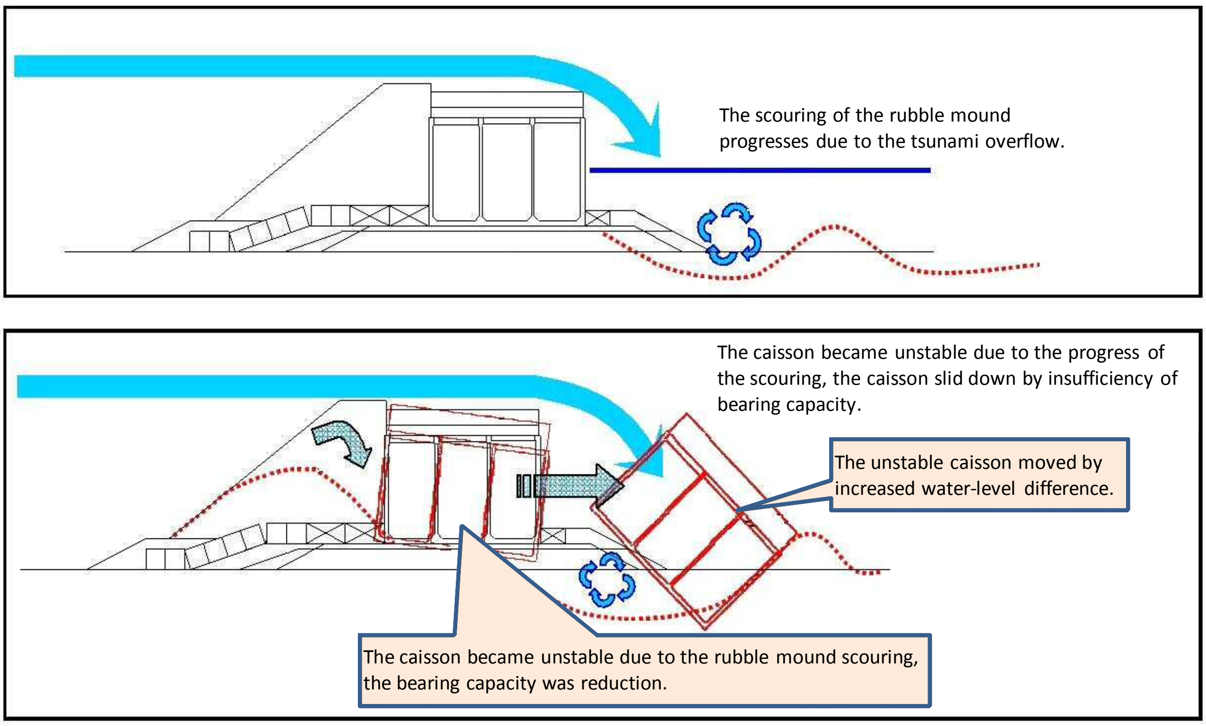

Figure 23. Mechanism of breakwater collapse by Tsunami overflow (MLIT, 2011)

5.1 Outline of Experiment

Experiments used a wave flume of 50m long, 1m wide and 1.5m deep in Ujigawa Open Laboratory, DPRI, Kyoto Univ., as shown in Figure 24. An overview of the experimental set-

up is shown in Figure 25. The bottom slope is formed as the water depth is shallow toward the breakwater model. The breakwater model was placed on a flat bottom. The width of the flume was reduced from 1*m* at offshore to 30*cm* at the breakwater to exert a big tsunami to the breakwater.
Table 5 lists the heights of the generated solitary waves. Initially small tsunami was generated and it was increased step by step. Table 6 shows the size of experimental materials. A model scale was 1/40. An overflow depth is more important than the tsunami height in front of the breakwater for affection of the tsunami overflow to the mound scouring. Therefore the tsunami overflow depth was same for the SPF and the mound heightening in the experiment. Figure 26 shows the cross-sectional view of the SPF and the rubble mound heightening. The SPF of 20*t*-type was set in 3 rows behind the breakwater and only the SPF closest to the breakwater was double. Armor blocks of 8*t*-type were installed on rubble mound slope part and on the sea bottom in some extent. In the mound heightening, core part was formed by the

Figure 24. Wave flume

Table 5. Size of solitary waves

Step	Wave height in front of breakwater	
	Model scale(cm)	Actual scale(m)
1	16	6.4
2	18	7.2
3	20	8.0
4	22	8.8
5	24	9.6
6	26	10.4

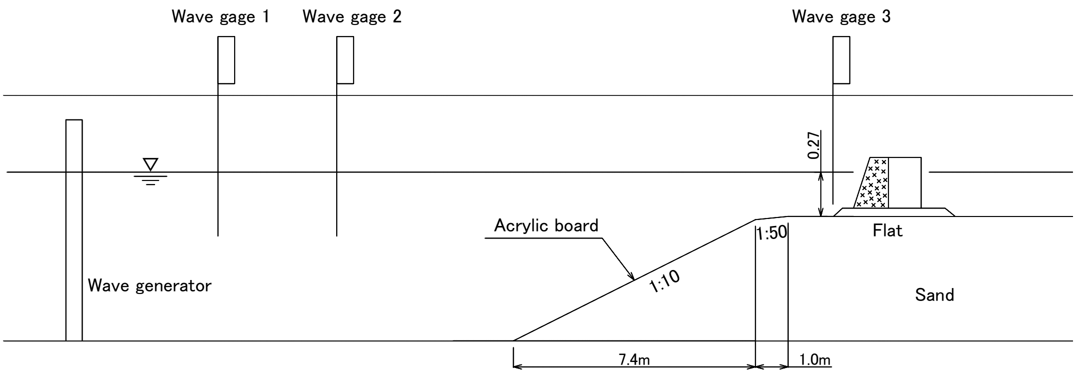

Figure 25. Overview of the experiment

Table 6. Size of experimental materials

	Model scale		Actual scale	
	Size	Mass	Size	Mass
Caisson	H31cm*B20.5cm*L15cm	18.2kg	H12.4m*B8.2cm*L6.0m	1,165t
Foundation rubble mound	φ10 to φ13mm	1 to 3g	φ40 to φ50cm	100 to 200kg
Armour stone (exist)	about φ15mm	5g	about 60cm	300kg
Armour stone (new)	about φ33mm	51g	about 1.35m	3.3t
CWB	L7.5cm*B7.5cm*H3.25cm	305g	L3.0m*B3.0m*H1.5m	19.48t
Inner stone (for CWB)	about φ15mm	5g	about 60cm	300kg

same size gravels as rubble mound and covered with 2 layers armor stones of about 40g. The cross section (a) of the SPF and armor block was designed to be approximately the same sliding resistant force and construction cost with the cross section (b) of the mound heightening.

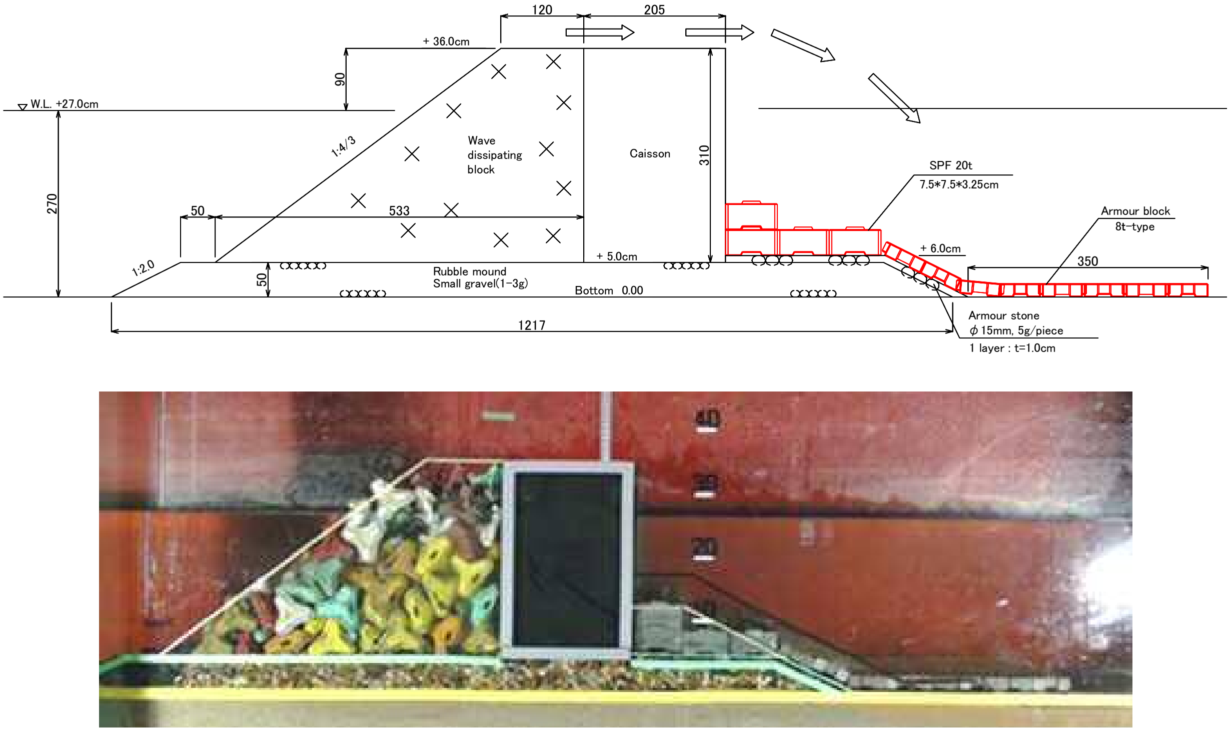

(a) SPF and Armor block

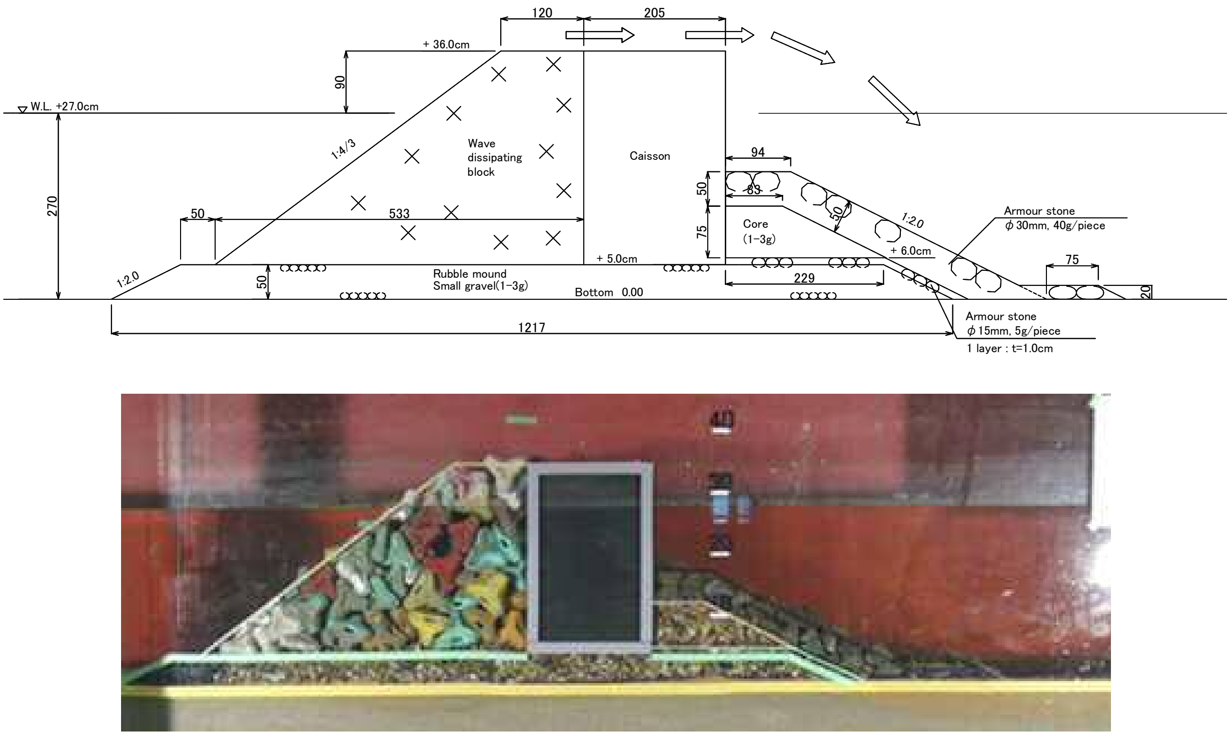

(b) Rubble mound heightening

Figure 26. Cross-sectional view

5.2 Experimental Result

Table 7 and Figure 27 show the experimental results. The vertical and horizontal axis of Figure 27 are the damage ratio and tsunami overflow depth, respectively. The solitary waves were set to become approximately the same overflow depth. The damage ratio was calculated as (decreased area) / (original area). The removal of inner stones of the SPF also was counted as the damage.

The results of the SPF, the damage ratios from Step3 to Step6 were small as 0.4% to 2.6% in the plane and 1.3% to 6.4% in the cross section. These damages were caused by slight removal of the inner stones. The armor blocks at the tip were slightly moved due to the tsunami overflow in Step7, but the SPF itself did not move at all. The entire armor blocks were damaged in Step8 and the SPF farthest row from caisson was slightly slid.

The results of the mound heightening shows that the damage of 1% in the plane and 3.8% in the cross section occurred in Step1 because surface armor stones were washed away by small overflow. The core part was eroded in Step6 of the overflow depth 13.0*cm* although the damage occurred only in armor stones until Step5. The core began to erode by the flow which gradually come close to the caisson when overflow gradually reduced. The sliding resistant force is not kept when the core is damaged. The mound heightening was ended at Step6.

Table 7. Experimental results

Case	Maximum wave height in front of breakawter (cm)	Overflow depth (cm)	Damage ratio(%)	
			Plane	Cross-section
SPF-Step1	16.3	4.0	0.0	0.0
SPF-Step2	20.0	7.5	0.0	0.0
SPF-Step3	19.6	7.5	0.8	2.2
SPF-Step4	21.4	9.0	0.4	1.3
SPF-Step5	23.0	11.0	1.6	3.1
SPF-Step6	24.9	13.0	2.6	6.4
SPF-Step7	26.8	14.0	3.3	12.6
SPF-Step8	27.7	17.5	24.2	16.9
MHM-Step1	15.9	3.5	1.0	3.8
MHM-Step2	18.0	5.5	1.0	2.2
MHM-Step3	20.2	7.5	2.5	4.5
MHM-Step4	22.7	9.8	6.8	9.5
MHM-Step5	24.4	11.5	24.6	13.0
MHM-Step6	25.7	13.0	65.0	33.3

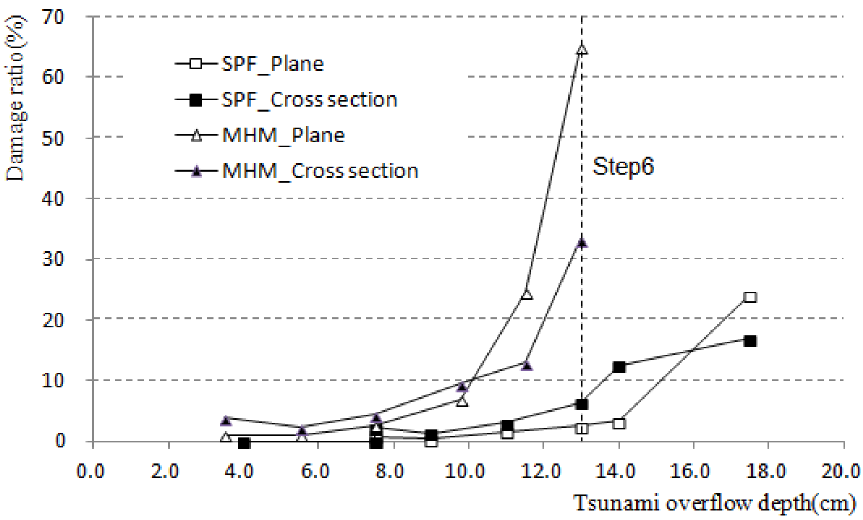

Figure 27. Relationship between the tsunami over flow and damage ratio

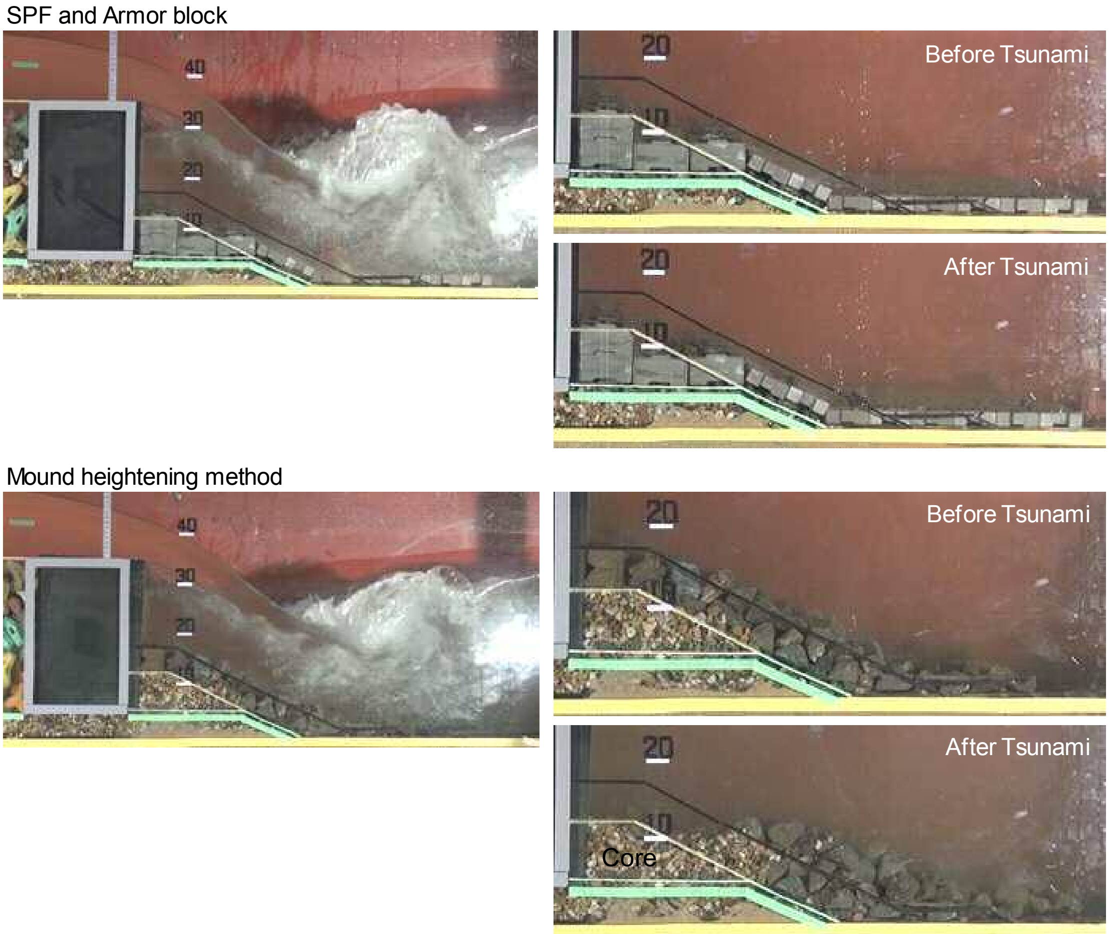

Figure 28. Experimental result of the cross section of Step6

Figure 28 shows the experimental result of the cross section in Step6. The core of the mound heightening was scoured significantly as the cross sectional damage 33.3%. On the other hand, the SPF did not move at all although the small damage of 6.4% occured due to the slightly runoff of the inner stones.

5.3 Advantage of the SPF

The damage ratio in both the plane and cross section of the mound heightening were less than 10% until Step4, but they became more than 10% at Step5. After that they exceeded 20% at Step6 and the core was eroded.

On the other hand, the damage ratio of both the plane and cross section of the SPF and armor block were less than 10% at Step6. The both damage ratios became more than 15% at Step8, because many armor blocks moved. The SPF itself was almost not damaged even at large overflow depth in Step7 and 8. It is thought that the forces of the overflow and uplift did not affect the SPF because of the hole of the SPF.

There are a number of parameters like the water depth or mound width in the tsunami overflow experiment, and it is necessary to conduct the experiment under various conditions. However, the stability performance of the SPF obtained from this experiments is quite high, it is found that the SPF is more effective on the breakwater reinforcement against tsunami overflow than the mound heightening.

6. CONCLUSION

The present paper has investigated applicability of the counter-weight type concrete block named *SUBPLEO FRAME* to reinforcement of the upright breakwater against the tsunami and extremely big wave. The design friction factor was determined as 0.75 through the pulling experiments of the block models. The hydraulic model experiments confirmed the validity of the value of the friction factor.
The determination procedure of the necessary number of SPF has been proposed for the reinforcement of breakwater stability and the effectivity of the procedure was confirmed by the model experiments.
The tsunami overflow experiment was also carried out, it is found that the SPF has high stability performance and is effective on the breakwater reinforcement against tsunami overflow.

We have learnt a lot from Tohoku Earthquake Tsunami Disaster 2011.
Japan is an island country with many coastal structures. Among them, the number of upright breakwater is the most in the world. We hope that the SPF will be adopted in the many field.

The SPF is used actually as a reinforcement method of breakwater at Hachinohe port.

7. ACKNOWLEDGEMENT

The SPF was developed by joint research with Disaster Prevention Research Institute, Kyoto University. I would like to express appreciation to Prof. Tetsuya HIRAISHI for his guidance and advice. I would also like to appreciate to the student of Kyoto Univ., Mr. Tatsuya KAWATA, for his big support on the experiments and analyses.
I would like to express my sincere gratitude to the councilor of Coastal Development Institute of Technology, Dr. Tomotsuka TAKAYAMA and the secretary general of PIANC-Japan, Dr. Tadahiko YAGYU, for their useful advice.
I would like to thank to president of NIKKEN KOGAKU CO., LTD., Mr.Takaki YUKIMOTO, senior corporate adviser, Mr. Yukio NISHIDA and corporate adviser, Mr. Hisao OUCHI for I had been given by them the opportunity to write this paper under their big support.

8. REFERENCES

TECHNICAL STANDARDS AND COMMENTARIES FOR PORT AND HARBOUR FACILITIES IN JAPAN (2009), OCDI, 606p and 358p.

Takeshi HORIE, Kenichiro MINAMI, Kensuke KAWAZUMI and Tadashi OHTSUKI. (1995), "Pilot Experiments on Coastal Water Purification by Stone Bed with Biofilm", Proc. 23th Japanese Conf. Environmental Systems, pp.390-401(in Japanese).

Kenichiro SHIMOSAKO and Shigeo TAKAHASHI. (1998), "Reliability Design Method of Composite Breakwater using Expected Sliding Distance", Report of the port and harbour research institute, Vol.37, No.3.

Ministry of Land, Infrastructure and Transport Tohoku Regional Development Bureau Port and Airport Department (home page), http://www.pa.thr.mlit.go.jp/kakyoin/PDF/3shiryou.pdf, referred on July 30, 2012.

Tetsuya HIRAISHI, Katsuya HIRAYAMA, Hiroaki KASHIMA, Kazuto HARUO and Ichiro MIYAZATO. (2008), "Example and Characteristic of Disaster induced by Accidental Wave Load", Proc. 55th Japanese Conf. Coastal Eng., pp.981-985(in Japanese).

Tetsuya HIRAISHI, Hajime MASE, Tatsuya KAWATA, Takaki YUKIMOTO, Seishi TOKUNAGA and Hiroshi MATSUSHITA. (2011), "Experimental Study on Counter-weight Blocks for Breakwater Stability", Proc. 21th International Conference of Offshore and Polar Eng., Vol.3.